Eng. Sci., 2022, **19**, 253–261

Engineered Science

DOI: https://dx.doi.org/10.30919/es8e708

# Multi-metallic Nanosheets for High-performance Hydrogen Evolution Reaction

Xuchao Pan,[1,*] Zhikai Zheng,[1] Xinlai Zhang,[2] Xian He,[2,*] Yashuai An,[1] Yu Hao,[1] Kai Huang[2] and Ming Lei[2,*]

## Abstract

Communication-efficient and stable electrocatalysts for hydrogen evolution reaction (HER) are essential to building a new energy system based on clean energy by using electrolytic water for hydrogen production. As commercial Pt/C is limited in its application due to its cost and durability, the exploitation of high-performance, stable catalysts with high Pt utilization is crucial for the development of electrolytic water for the hydrogen production industry. Herein, we report a simple and reliable grinding-heating strategy to successfully construct the multi-metallic component nanosheets (PtRuMn), which exhibit excellent activity and good stability under both acidic and basic environments. The as-prepared PtRuMn showed excellent HER performance with a low overpotential of 41 mV (1 M KOH) or 36 mV (0.5 M $H_2SO_4$) to reach the current density of 100 mA $cm^{-2}$ and maintained approximately 95% of the initial current density after a 12 h chronoamperometry (CA) test. This work provides an effective method to improve the utilization of precious metals and to design and develop high-performance HER catalysts, which are important for the application of multiple types of electrolytic water devices at scale.

*Keywords:* Electrolytic water; High Pt utilization; Multi-metallic component; Nanosheet; High-performance HER catalysts.
Received: 18 April 2022; Revised: 10 May 2022; Accepted: 10 May 2022.
Article type: Research article.

## 1. Introduction

Along with the global industrial restructuring and industrial upgrading, energy development and utilization technologies are undergoing profound changes, and green energy is gradually becoming a global energy development trend.[1-5] Hydrogen was considered to be the most ideal vehicle to promote the clean and efficient use of traditional fossil energy and even to support the large-scale development of renewable energy due to its wide source, high calorific value, clean and carbon-free, flexible, and efficient characteristics.[6-12] Among the various ways to obtain hydrogen sources, electrocatalytic water is considered an effective route given its low energy consumption, environmentally friendly handling, and high product purity.[13-19] One key aspect of this technology is the development of hydrogen evolution reaction (HER) electrocatalysts that must be both active and stable under acidic and alkaline media.[20-25] In the reported electrocatalysts, platinum (Pt) and platinum group metals are the most effective catalysts for HER, but their large-scale commercial utilization is restricted by their scarcity and high cost.[26-30] Therefore, it is necessary to design effective strategies to develop high-performance electrocatalysts with high Pt utilization and low cost.[31]

One attractive strategy for solving this problem is the construction of two-dimensional nanostructures.[32-37] Two-dimensional nanomaterials possess a high specific surface area, many low-coordination defect atoms, and unique structural properties for significantly enhanced catalyst activity.[38-41] Another effective approach is to partially displace Pt with a less expensive metal. Ruthenium (Ru) has shown great potential to be an alternative HER catalyst because of its similar metal–hydrogen bonding (M-$H_{ads}$) bond energy as Pt and its lower price.[42-52] For example, Dang *et al* reported the accurate tuning of Ru-H binding energy to obtain high-performance HER catalysts Ru/$RuO_2$.[45] The third way to improve the performance of Pt-based catalysts is doping with transition metals, which not only reduces the precious metal loading to lower the electrode cost, but also further adjusts the electronic energy band structure, local charge distribution, and carrier density to enhance catalytic activity and stability.[53-62] Although many catalysts have been constructed based on the single strategy described above, there is still a paucity of

[1] *Ministerial Key Laboratory of ZNDY, Nanjing University of Science &Technology, Nanjing 210094, China.*
[2] *State Key Laboratory of Information Photonics and Optical Communications, School of Science, Beijing University of Posts and Telecommunications, Beijing 100876, China.*
**E-mail:* pxchxc@njust.edu.cn (X. C. Pan); mlei@bupt.edu.cn (M. Lei); yqwsn@bupt.edu.cn (X. He)

research on the integration of two-dimensional structures and trimetallic components into HER catalysts.[63-70]

Herein, we report a facile and reliable strategy for the construction of multi-metal oxide nanosheets. The efficient synthesis of multi-metal oxide nanosheets is achieved by heating the ground metal precursors. To systematically investigate the influence of different compositions on the catalytic performance mechanisms, nanosheets with different compositions were prepared using different metal precursors under the same preparation parameters. Further, morphology, structure, and HER catalytic activity were investigated in detail using a series of structural and performance characterizations to refine the mechanism of enhanced HER catalytic performance by multi-metallic components and two-dimensional structures. The results show that the construction of two-dimensional nanosheet structures and polymetallic components effectively improves the utilization of noble metal atoms and exposes more defective atoms and active sites in the catalyst, leading to excellent HER activity and stability in acidic and alkaline environments. Among them, the nanosheets (PtRuMn) prepared with three metal precursors (Pt, Ru, and Mn) showed the best HER activity, with overpotentials of only 41 (1.0 M KOH) or 36 mV (0.5 M $H_2SO_4$) at a current density of 100 mA $cm^{-2}$ and good stability in both media. This work provides an attractive research direction for the development of high-performance HER catalysts for acid-base general-purpose applications.

## 2. Experimental section

### 2.1 Material

Platinum acetylacetonate ($Pt(C_5H_7O_2)_2$, Aladdin), ruthenium acetylacetonate ($C_{15}H_{21}O_6Ru$, Aladdin), manganese acetylacetonate ($MnC_{15}H_{21}O_6$, Aladdin), and potassium bromide (KBr, Aladdin) were used as received without any further purification.

### 2.2 Preparation of catalyst samples

The platinum acetylacetonate (0.5 mmol), manganese acetylacetonate (0.5 mmol), ruthenium acetylacetonate (0.5 mmol), and potassium bromide (6 mmol) were dissolved in aqueous ethanol (ethanol: ultrapure water = 6:1). The solution was then poured into a mortar and ground until the solvent evaporated completely, after which the powder mixture was collected and laid flat in a porcelain boat. Then the porcelain boat was heated in a preheated muffle furnace (muffle temperature: 290 °C) for 90 min and then removed. Finally, PtRuMn was rinsed with deionized water and ethanol and then dried at room temperature to obtain PtRuMn. In addition, PtRu and PtMn nanosheets were prepared by only changing the type of precursors.

### 2.3 Characterization

An X-ray diffractometer (XRD, D/max 2500 V) was applied to examine the crystal structure of the samples. The morphology and energy dispersion spectroscopy (EDS) elemental mapping images of samples was analyzed using transmission electron microscopy (a JEM-2100F). To study the surface chemistry of these samples X-ray photoelectron spectroscopy (Escalab 250 Xi) was used.

### 2.4 Electrochemical measurements

All electrochemical measurements were performed with an Autolab PGSTAT-204 potentiostat equipped with Nova 2.13 software. The HER performance of the catalysts was described using a conventional three-electrode electrochemical system in $N_2$-saturated 1.0 M KOH or 0.5 M $H_2SO_4$ electrolytes. The working electrode was prepared by the following procedure: catalysts (5 mg) were dispersed in a mixture of alcohol (250 μL), water (700 μL), and Nafion solution (50 μL, 5%) for 20 min to form homogeneous catalyst inks. Then a certain amount of the catalyst ink was pipetted onto the surface of conductive carbon paper by several times so that the density of the catalyst on the surface of conductive carbon paper is 1 mg $cm^{-2}$. The counter electrode was a graphite rod and the reference electrodes were Hg/HgO (1.0 M KOH) and Ag/AgCl (0.5 M $H_2SO_4$), respectively. All potentials applied in 1.0 M KOH were calibrated to RHE using the following equation: $E_{RHE} = E_{Hg/HgO} + 0.098 + 0.059\times$ pH and all potentials applied in 0.5 M $H_2SO_4$ were calibrated to RHE using the following equation: $E_{RHE} = E_{Ag/AgCl} + 0.197 + 0.059 \times$ pH. For linear scanning voltammetry (LSV) measurements were performed with a sweep rate of 5 mV $s^{-1}$, before which more than 30 cycles of cyclic voltammetry (CV) were performed to activate the prepared catalysts with a sweep rate of 50 mV $s^{-1}$. The apparent Tafel slope was derived from the *IR*-corrected polarization curve by fitting experimental data to the equation $\eta = a + b * \log|j|$, where $\eta$ is the *IR*-corrected potential, $a$ is the Tafel constant, $b$ is the Tafel slope, and $j$ is the current density. The electrochemical impedance spectroscopy (EIS) tests were measured by AC impedance spectroscopy at -0.1 V with a frequency ranging from $10^5$ Hz to 0.1 Hz. An accelerating stability measurement was evaluated using 1000, 2000, and 5000 continuous cycles from -0.05 to 0.2 V at a scan rate of 50 mV/s. The ECSA values were measured through CV in the selected non-faradaic range. The current densities have a linear relationship against different scan rates (10-60 mV/s) and the values of the slop were considered as twice Cdl. CA tests were performed at a constant voltage of -1.002 V (vs. Hg/HgO) or -0.254 V (vs. Ag/AgCl) for 12 h in $N_2$-saturated 1.0 M KOH or 0.5 M $H_2SO_4$, separately. All polarization curves were 95% *iR*-corrected, all potentials were referenced to RHE and all measurements were performed at room temperature.

## 3. Results and discussion

### 3.1 Synthesis and morphology

We propose a grinding-heating strategy for the synthesis of multi-metallic nanosheet catalysts to achieve an effective combination of multi-metallic components and two-dimensional structures. As shown in Fig. 1a, the three metal

 

precursor powders were firstly dispersed homogeneously by grinding, and then the ground powders were heated in a muffle furnace at 290 °C for 90 min. The heated powder was rinsed with deionized water and ethanol and dried at room temperature to obtain PtRuMn. Both morphological and microstructural aspects of the PtRuMn catalyst were investigated by TEM. Figs. 1b-e shows TEM images of the PtRuMn catalyst at different magnifications, indicating that PtRuMn exhibits a two-dimensional nanosheet morphology. The lattice stripe spacing in the HR-TEM image (Fig. 1d) doesn't correspond to any one of Pt, Ru, and Mn, which we speculate that the introduction of Ru and Mn into the lattice of Pt may result in a change in the crystal plane spacing as reported.[71] Furthermore, Figs. 1f-i displays the corresponding elemental mapping images of PtRuMn, confirming the presence and uniform distribution of Pt, Ru, Mn, and O elements in PtRuMn nanosheets. According to the TEM results, the catalyst (PtRuMn) possesses three metal elements and nanosheet characteristics.

### 3.2 Structural characterizations

The XRD pattern of PtRuMn shows three strong diffraction peaks at 40.00°, 46.54°, and 67.88°, located between the peaks of standard Pt (PDF# 04-0802) and Ru (PDF# 88-2333) in Fig. 2a. The diffraction peaks of PtRuMn are shifted to higher angles in comparison to Pt/C, and this peak shift is suggested by previous studies to be caused by the alloying of PtRu. There are lattice field changes in PtRuMn and PtRu due to the similar electronegativity of Pt and Ru elements, with no transfer of valence electrons between them and only interaction between Ru and Pt atoms, causing lattice distortions.[71] Besides, the positive shift of the peaks implies the formation of compressive strain on the lattice, which is favorable for the adsorption/desorption of the reactants as well as for the catalytic enhancement. The weak $Mn_3O_4$ signals were also detected at 28.94°, 32.52°, and 36.10°, indicating the presence of Mn in PtRuMn in the form of $Mn_3O_4$.[72]

The XPS measurements were performed to further determine the electronic structure and elemental valence of the prepared catalysts. In Fig. 2b, the XPS survey spectra verified the presence of elements Pt, Ru, Mn, and O in the PtRuMn nanosheets. PtRuMn shows two peaks at 71.3 eV (Pt $4f_{7/2}$) and 74.6 eV (Pt $4f_{5/2}$) in Fig. 2c, which are negatively shifted by 0.3 and 0.2 eV in PtRu and PtMn, indicating that Pt in PtRuMn possesses a lower electron density and higher valence than in PtRu and PtMn. The peak at 71.3 eV can be deconvoluted into

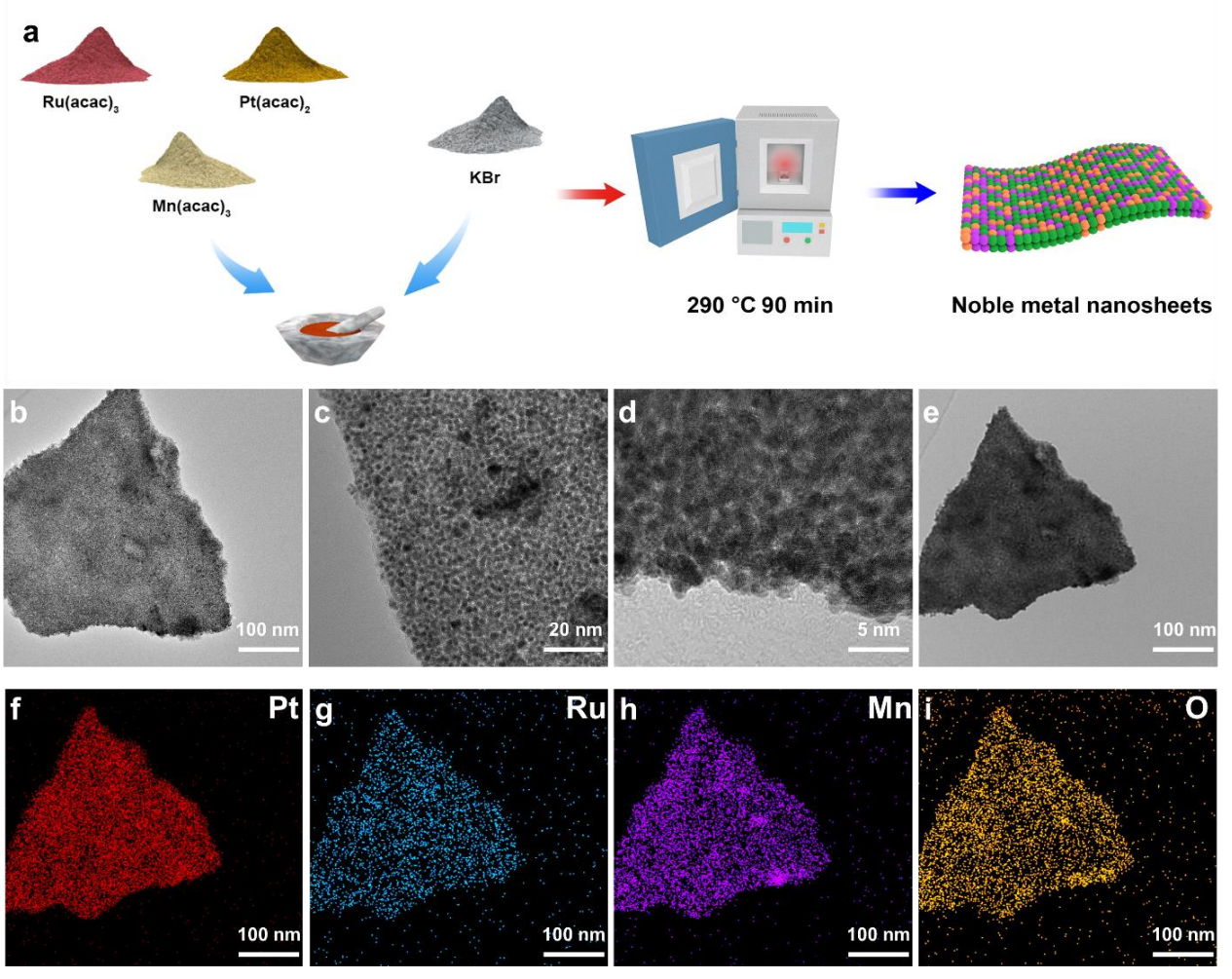


**Fig. 1** (a) The schematic illustration of the synthesis of PtRuMn. TEM images (b,e), HR-TEM images (c,d), and EDS elemental mappings (f-i) of PtRuMn.

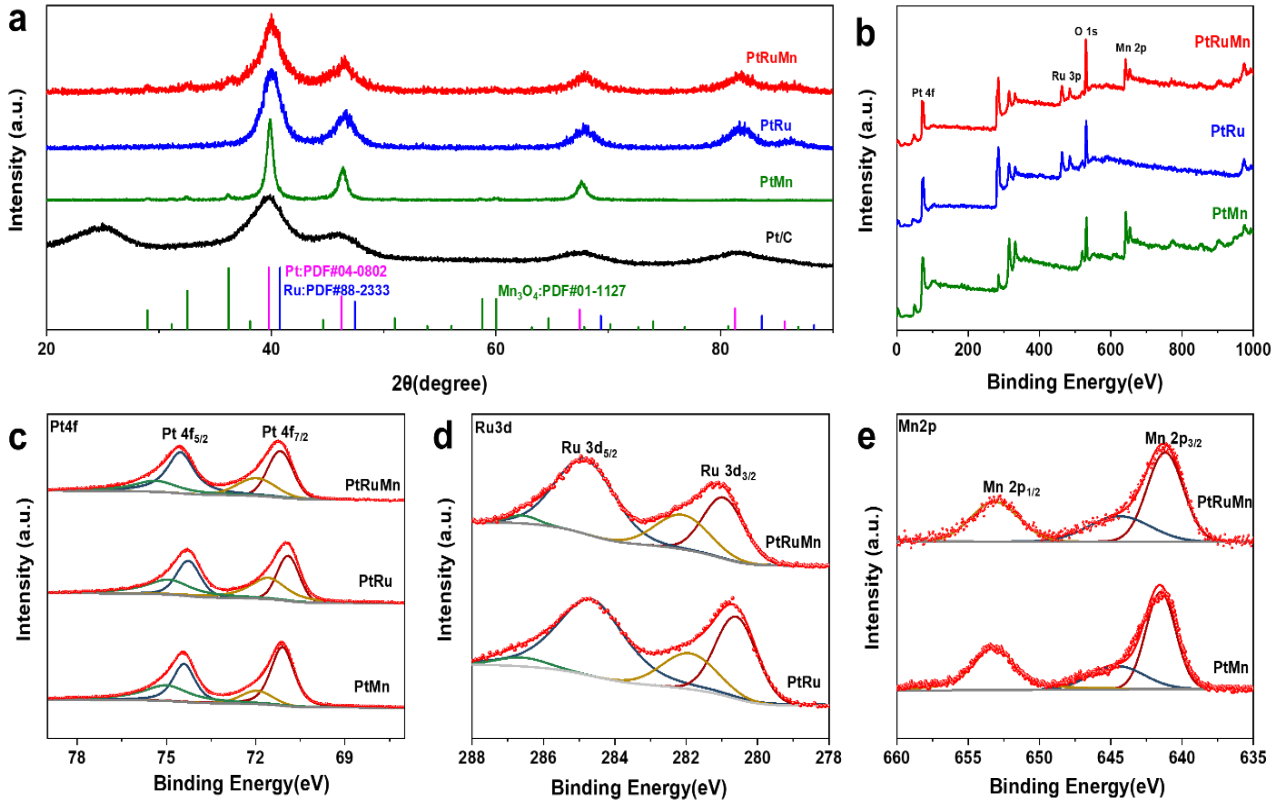


**Fig. 2** (a) XRD patterns of PtRuMn, PtRu, PtMn, and Pt/C catalysts. XPS spectra of(b) survey, (d) Pt 4f, (e) Ru 3d, and (f) Mn 2p for PtRuMn, PtRu, and PtMn.

two peaks at 71.2 eV ($Pt^0$) and 72.0 eV ($Pt^{2+}$), and the peak at 74.6 eV can be deconvoluted into two peaks at 74.5 eV ($Pt^0$) and 75.4 eV ($Pt^{2+}$).[71-74] The Ru 3d spectrum in Fig. 2d shows that the peaks located at 280.7 eV and 284.7 eV in PtRu correspond to Ru $3d_{5/2}$ and Ru $3d_{3/2}$, which can be deconvoluted to reveal peaks for $Ru^0$ (280.6 and 284.8 eV) and the partially oxidized Ru (282 and 286.7 eV). The XPS peaks of PtRuMn also exhibited a positive shift by 0.4 eV compared to PtRu, indicating that Ru in PtRuMn possesses a higher valence than in PtRu.[73] Fig. 2e presents the Mn 2p spectrum of PtRuMn at about 641.6 eV and 653.2 eV with peaks in the Mn 2p spectrum attributed to Mn $2p_{3/2}$ and Mn $2p_{1/2}$, the peak at 644 eV can be decomposed into two peaks at 641.5 eV ($Mn^{3+}$) and 646.4 eV ($Mn^{4+}$), while the signal at 653.2 eV corresponds to $Mn_3O_4$. The PtRuMn XPS peak has a negative shift by about 0.3 eV compared to PtMn, which implies the decrease of the chemical valence of Mn.[72,75,76] These XPS analyses revealed that PtRuMn has the strongest interaction between the metal atoms and that some Ru and Pt atoms are partially oxidized because of the charge transfer to Mn atoms.

### 3.3 Electrochemical characterization

The HER performance of the prefabricated catalysts under both the acidic and alkaline conditions was first evaluated. Fig. 3a and Fig. 3d show the polarization curves recorded by linear sweep voltammetry (LSV) for all electrodes at a scan rate of 5 mV $s^{-1}$ in $N_2$-saturated 1 M KOH electrolyte and 0.5 M $H_2SO_4$ electrolyte. The results showed that PtRuMn exhibited the best HER activity in alkaline electrolytes, with overpotentials of 8 mV and 41 mV at current densities of 10 mA $cm^{-2}$ and 100 mA $cm^{-2}$, which were smaller than those of PtRu (20 mV, 86 mV), PtMn (113 mV, 308 mV) and the commercial catalyst Pt/C (38 mV, 163 mV), indicating that the polymetallic fraction could enhance HER activity. Similar results were obtained in the acidic electrolyte, where PtRuMn achieved current densities of 10 mA $cm^{-2}$ and 100 mA $cm^{-2}$ with low overpotentials of 6 mV and 36 mV, superior to PtRu (26 mV, 65 mV), PtMn (33 mV, 77 mV) and Pt/C (26 mV, 81 mV) catalysts (Fig. 3d). The Tafel slopes and charge-transfer resistances of these electrodes were investigated in acidic and alkaline environments to gain insight into the HER kinetic mechanism. Fig. 3b and Fig. 3e show that PtRuMn both exhibited the smallest Tafel slopes of 20.11 mV $dec^{-1}$ (0.5 M $H_2SO_4$) and 27.61 mV $dec^{-1}$ (1 M KOH), which are lower than PtRu (26.92 mV $dec^{-1}$, 50.96 mV $dec^{-1}$), PtMn (36.21 mV $dec^{-1}$, 100.99 mV $dec^{-1}$) and Pt/C (27.88 mV $dec^{-1}$, 60.14 mV $dec^{-1}$), suggesting that the water dissociation kinetics have been substantially enhanced after the introduction of Ru and Mn. The electrochemical impedance spectroscopy (EIS) Fig. 3c and Fig. 3f show that PtRuMn presents the smallest semicircle associated with the charge-transfer resistance, which indicates the lowest charge-transfer resistance in both acidic and alkaline conditions, one of the key factors affecting HER kinetics. The above results demonstrate that the enhancement of HER catalytic performance can be brought about due to the electronic coupling and synergistic effect between the polymetallic

 

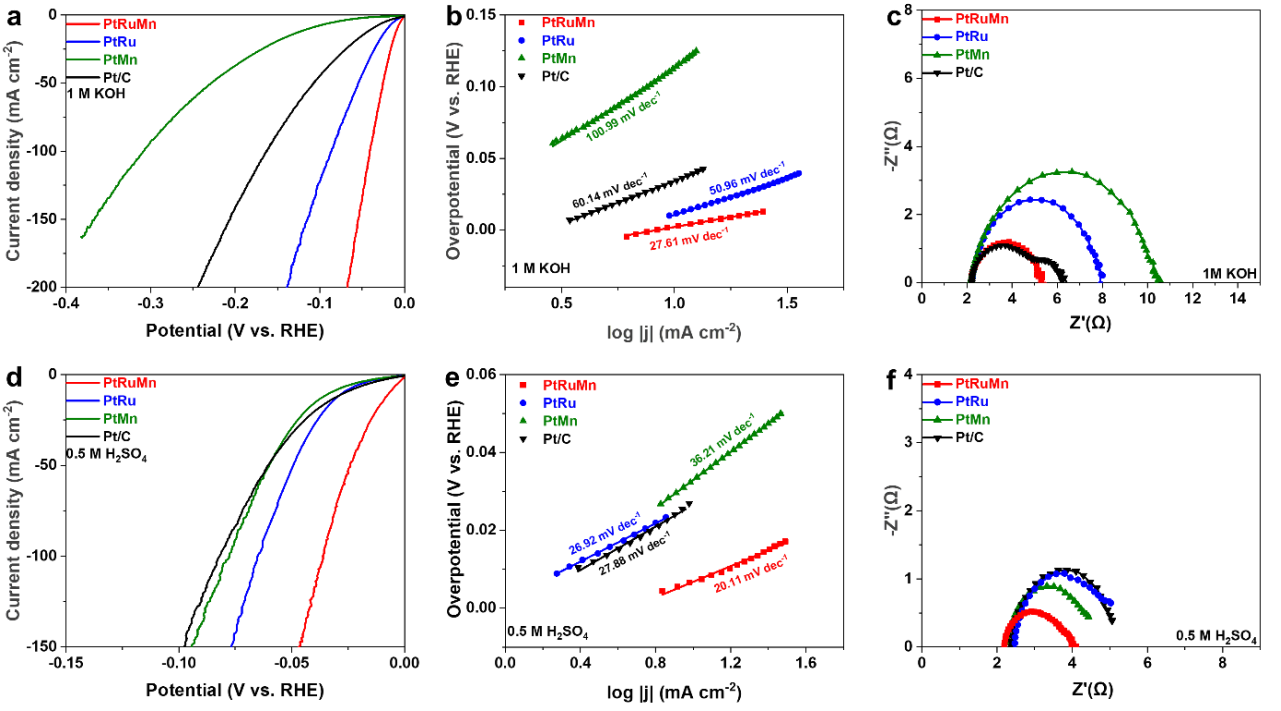


**Fig. 3** (a) LSV curves, (b) Tafel plots, and (c) Nyquist plots of PtRuMn, PtRu, PtMn, and Pt/C in 1.0 M KOH. (d) LSV curves, (e) Tafel plots, and (f) Nyquist plots of PtRuMn, PtRu, PtMn and Pt/C in 0.5 M $H_2SO_4$.

components.

Then, we fixed the heating temperature of the muffle furnace and changed the heating atmosphere to investigate the effect. We found that the overpotential, Tafel slope, and charge transfer resistance of PtRuMn-Ar are bigger under both the acidic and alkaline conditions when protective gas (Ar) was used during the heating process (Fig. 4). This reflects that the presence of $O_2$ during the heating process can maximize the formation of metal-oxide-metal bonds in the samples thus enhancing the HER activity.

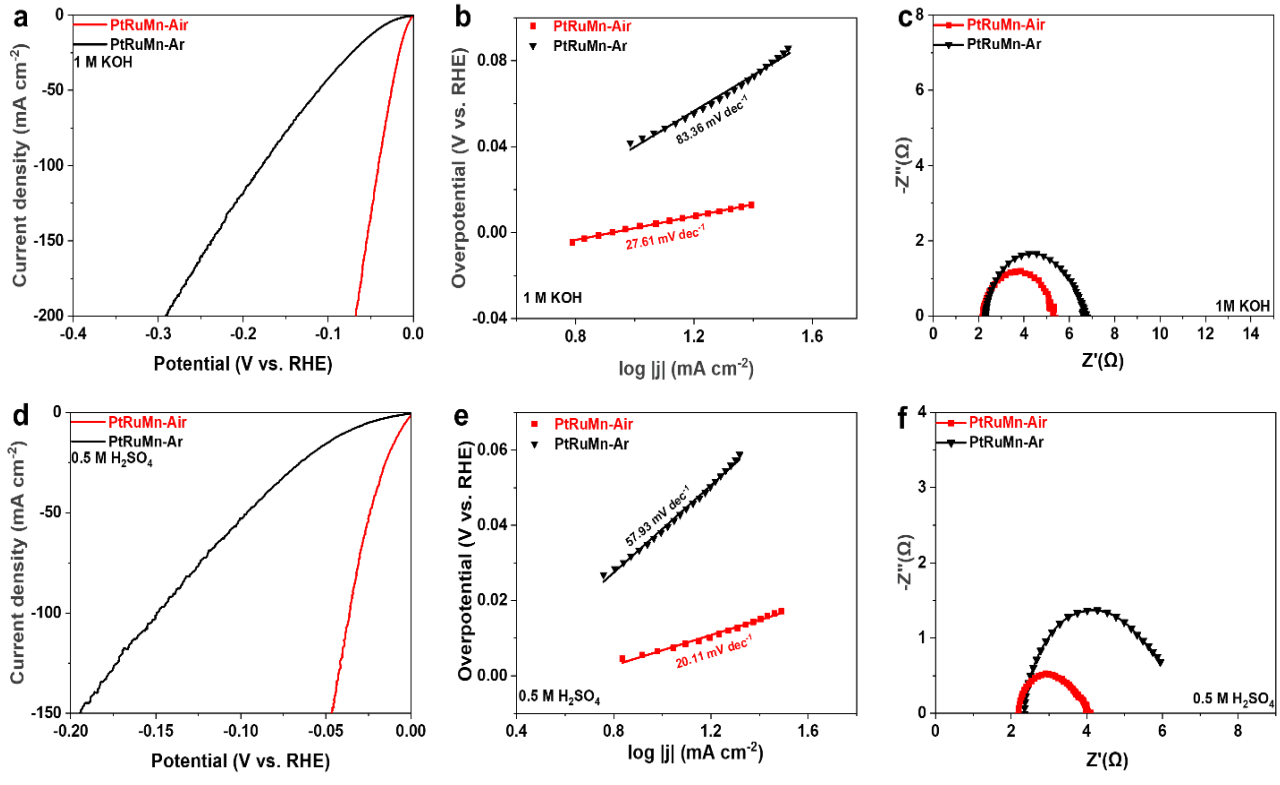


**Fig. 4** (a) LSV curves, (b) Tafel plots, and (c) Nyquist plots of PtRuMn-Air and PtRuMn-Ar in 1.0 M KOH. (d) LSV curves, (e) Tafel plots, and (f) Nyquist plots of PtRuMn-Air and PtRuMn-Ar in 0.5 M $H_2SO_4$.

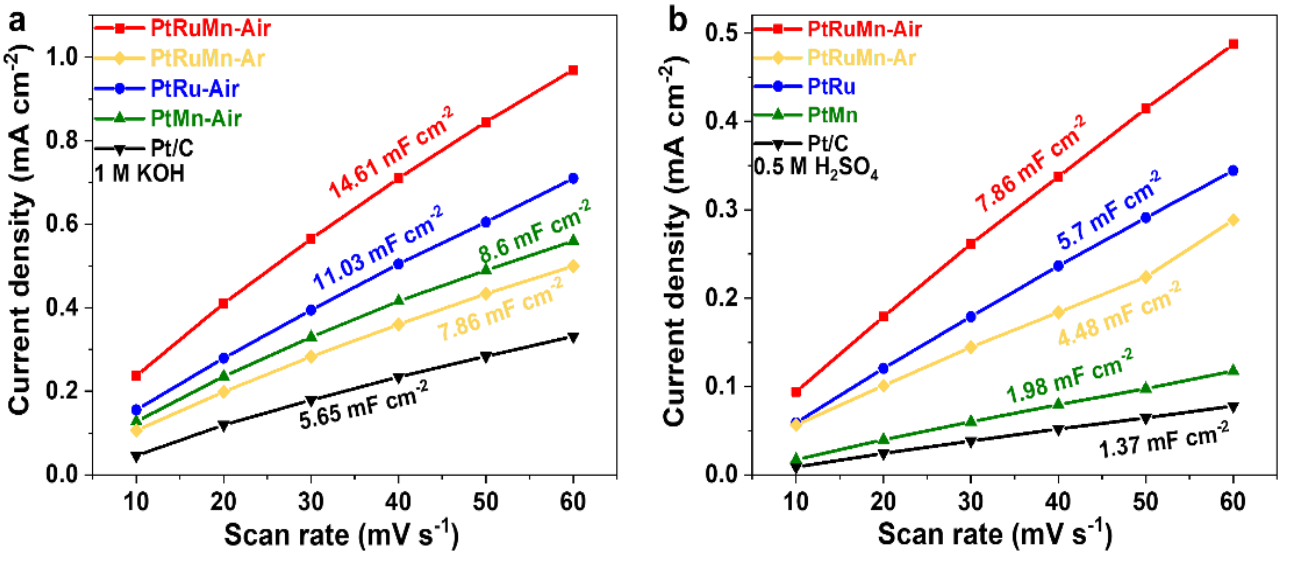


**Fig. 5** (a) current density versus scan rate plot of PtRuMn, PtRu, PtMn, and Pt/C in 1.0 M KOH. (b) current density versus scan rate plot of PtRuMn, PtRu, PtMn, and Pt/C in 0.5 M $H_2SO_4$.

As electrochemical active surface area (ECSA) is also one of the major factors affecting HER performance, we evaluated the ECSA of the catalysts by the double-layer capacitance ($C_{dl}$) in alkaline or acidic environments, and $C_{dl}$ has further obtained from the cyclic voltammetry (CV) curves of the catalysts (Fig. S1 and Fig. S2). The $C_{dl}$ values of PtRuMn, PtRu, and PtMn with two-dimensional structures are larger than Pt/C catalysts, suggesting that the two-dimensional structures provide a larger active area for the catalysts (Figs. 5a and b), this result is as expected from our design of the catalyst structures.

In addition, we examined the stability of PtRuMn in acidic and alkaline conditions by ADT, which showed negligible degradation after 1000, 2000, and 5000 CV cycles (Figs. 6a and c). PtRuMn was measured in CA tests for 12 h under both the acidic and alkaline conditions, further demonstrating its excellent stability (Figs. 6b and d).

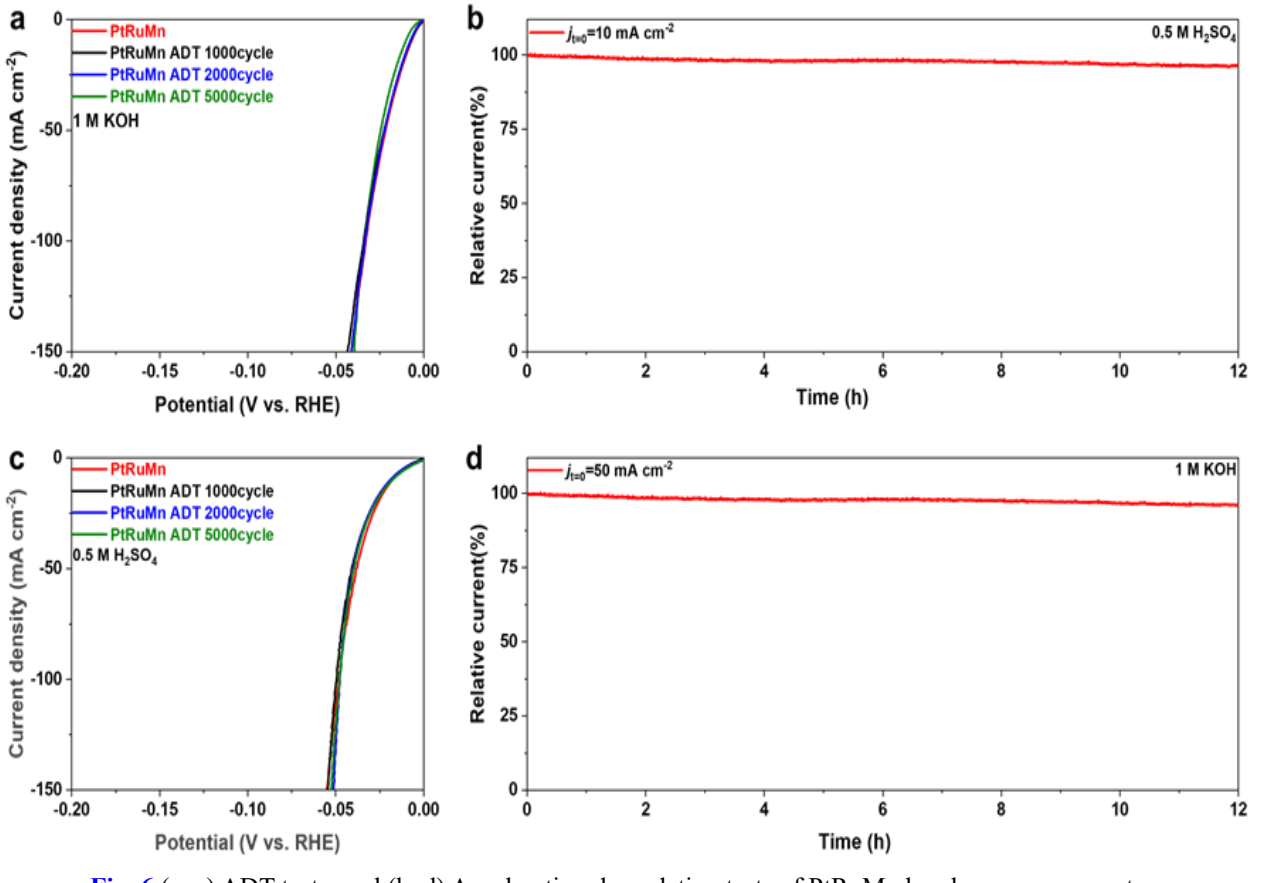


**Fig. 6** (a, c) ADT tests, and (b, d) Accelerating degradation tests of PtRuMn by chronoamperometry.

 

## 4. Conclusions

In summary, we have developed a simple and reliable grinding-heating preparation process and successfully synthesized multi-metallic component nanosheet materials. Based on the special morphological structure and the synergistic interaction between the multi-metal components, the PtRuMn exhibits excellent HER activity in both acidic and alkaline environments, with overpotentials of 41 mV (1 M KOH) or 36 mV (0.5 M $H_2SO_4$) at a current density of 100 mA $cm^{-2}$ and small Tafel slopes of 27.61 mV $dec^{-1}$ (1 M KOH) or 20.11 mV $dec^{-1}$ (0.5 M $H_2SO_4$). Experiments also demonstrated its long-term stability in acidic and alkaline environments. Thus, this work paves a promising way to improve the utilization of precious metals and to design and develop versatile high-performance catalysts.

This study is supported financially by the Support program for innovation and development of key industries in southern Xinjiang(2019DB011)

## Acknowledgments

This study was supported financially by the Fundamental Research Funds for the Central Universities (2021XD-A04-1), the Support program for innovation and development of key industries in southern Xinjiang (2019DB011), the National Natural Science Foundation of China (Nos.61974011and 51902027), the Fund of State Key Laboratory of Information Photonics and Optical Communications (Beijing University of Posts and Telecommunications, P. R. China).

## Conflict of Interest

The authors declare no conflict of interest.

## Supporting information

Applicable.

## Reference

[1] J. Turner, *Science*, 2004, **305**, 972-974, doi: 10.1126/science.1103197.

[2] K. Huang, R. Wang, S. Zhao, P. Du, H. Wang, H. Wei, Y. Long, B. Deng, M. Lei, B. Ge, H. Gou, R. Zhang, H. Wu, *Energy Storage Materials*, 2020, **29**, 156-162, doi: 10.1016/j.ensm.2020.03.026.

[3] M. Chhetri, M. Rana, B. Loukya, P. Patil, R. Datta, U. Gautam, *Advanced Materials*, 2015, **27**, 4430-4437, doi: 10.1002/adma.201501056.

[4] X. Hu, H. Wu, S. Liu, S. Gong, Y. Du, X. Li, X. Lu, J. Qu, *Engineered Science*, 2022, **17**, 1-27, doi: 10.30919/es8d474.small.

[5] (a) N. Armaroli, V. Balzani, *ChemSusChem*, 2011, **4**, 21-36, doi: 10.1002/cssc.201000182. (b) S. Lamaison, D. Wakerley, *Nature Catalysis*, 2022, **5**, 242-243, doi: 10.1038/s41929-022-00774-7.

[6] Z. Zhao, H. Chang, R. Wang, P. Du, X. He, J. Yang, X. Zhang, K. Huang, D. Fan, Y. Wang, X. Pan, M. Lei, *Small Structures*, 2021, **2**, 2100069, doi: 10.1002/sstr.202100069.

[7] A truly sustainable future, *Nature Sustainability*, 2022, **5**, 281, doi: 10.1038/s41893-022-00892-x.

[8] G. Roymahapatra, M. Dash, S. Sinha, G. De, Z. Guo, *Engineered Science*, 2022, **19**, 114-124, doi: 10.30919/es8d671.

[9] M. Niu, K. Sui, X. Wu, D. Cao, C. Liu, *Advanced Composites and Hybrid Materials*, 2022, **5**, 450-460, doi: 10.1007/s42114-021-00296-z.

[10] F. Liu, Y. Zhao, H. Hou, Y. Zhao, Z. Wang, Z. Huang, *Advanced Composites and Hybrid Materials*, 2021, **4**, 1343-1353, doi: 10.1007/s42114-021-00347-5.

[11] A. Midilli, M. Dincer, M. Rosen, *Renewable and Sustainable Energy Reviews*, 2005, **9**, 255-271, doi: 10.1016/j.rser.2004.05.003.

[12] M. Momirlan, T. Veziroglu, *Renewable and Sustainable Energy Reviews*, 2002, **6**, 141-179, doi: 10.1016/s1364-0321(02)00004-7.

[13] K. Huang, S. Guo, R. Wang, S. Lin, N. Hussain, H. Wei, B. Deng, Y. Long, M. Lei, H. Tang, H. Wu, *Chinese Journal of Catalysis*, 2020, **41**, 1754-1760, doi: 10.1016/s1872-2067(20)63613-0.

[14] J. Su, Y. Yang, G. Xia, J. Chen, P. Jiang, Q. Chen, *Nature Communications*, 2017, **8**, 16028, doi: 10.1038/ncomms14969.

[15] T. Nielsen, *Catalysis Today*, 2005, **106**, 293-296, doi: 10.1016/j.cattod.2005.07.149.

[16] C. Lai, Y. Wang, L. Fu, H. Song, B. Liu, D. Pan, Z. Guo, I. Seok, K. Li, H. Zhang, M. Dong, *Advanced Composites and Hybrid Materials*, 2022, **5**, 536-546, doi: 10.1007/s42114-021-00375-1.

[17] F. Dawood, M. Anda, G. Shafiullah, *International Journal of Hydrogen Energy*, 2020, **45**, 3847-3869, doi: 10.1016/j.ijhydene.2019.12.059.

[18] X. He, S. Luan, L. Wang, R. Wang, P. Du, Y. Xu, H. Yang, Y. Wang, K. Huang, M. Lei, *Materials Letters*, 2019, **244**, 78-82, doi: 10.1016/j.matlet.2019.01.144.

[19] J. Turner, *Science*, 2004, 305, 972-974, doi: 10.1126/science.1103197.

[20] N. Dubouis, A. Grimaud, *Chemical Science*, 2019, **10**, 9165-9181, doi: 10.1039/c9sc03831k.

[21] G. Li, H. Jang, S. Liu, Z. Li, M. G. Kim, Q. Qin, X. Liu, J. Cho, *Nature Communications*, 2022, **13**, 1270, doi: 10.1038/s41467-022-28947-9.

[22] H. Tan, B. Tang, Y. Lu, Q. Ji, L. Lv, H. Duan, N. Li, Y. Wang, S. Feng, Z. Li, C. Wang, F. Hu, Z. Sun, W. Yan, *Nature Communications*, 2022, **13**, 2024, doi: 10.1038/s41467-022-29710-w.

[23] X. Zeng, Q. Luo, J. Li, Y. Li, W. Wang, Y. Li, R. Wu, D. Pan, G. Song, J. Li, Z. Guo, N. Wang, *Advanced Composites and Hybrid Materials*, 2021, **4**, 392-400, doi: 10.1007/s42114-021-00233-0.

[24] Z. Zhuang, W. Wang, Y. Wei, T. Li, M. Ma, Y. Ma, *Advanced Composites and Hybrid Materials*, 2021, **4**, 938-945, doi: 10.1007/s42114-021-00225-0.

[25] H. Wang, W. Fu, X. Yang, Z. Huang, J. Li, H. Zhang, Y. Wang, *Journal of Materials Chemistry A*, 2020, **8**, 6926-6956, doi: 10.1039/c9ta11646j.

[26] N. Cheng, S. Stambula, D. Wang, M. N. Banis, J. Liu, A.

Riese, B. Xiao, R. Li, T. Sham, L. Liu, G. Botton, X. Sun, *Nature Communications*, 2016, **7**, 13638, doi: 10.1038/ncomms13638.
[27] Z. Cao, Q. Chen, J. Zhang, H. Li, Y. Jiang, S. Shen, G. Fu, B. Lu, Z. Xie, L. Zheng, *Nature Communications*, 2017, **8**, 15131, doi: 10.1038/ncomms15131.
[28] K. Huang, Y. Xu, Y. Song, R. Wang, H. Wei, Y. Long, M. Lei, H. Tang, J. Guo, H. Wu, *Journal of Materials Science & Technology*, 2021, **65**, 1-6, doi: 10.1016/j.jmst.2020.04.065.
[29] K. Jiang, B. Liu, M. Luo, S. Ning, M. Peng, Y. Zhao, Y.-R. Lu, T. Chan, F. Groot, Y. Tan, *Nature Communications*, 2019, **10**, 1743, doi: 10.1038/s41467-019-09765-y.
[30] K. L. Zhou, Z. Wang, C. B. Han, X. Ke, C. Wang, Y. Jin, Q. Zhang, J. Liu, H. Wang, H. Yan, *Nature Communications*, 2021, **12**, 3783, doi: 10.1038/s41467-021-24079-8.
[31] X. Lu, J. Pan, E. Lovell, T. Tan, Y. Ng, R. Amal, *Energy & Environmental Science*, 2018, **11**, 1898-1910, doi: 10.1039/c8ee00976g.
[32] W. Zhang, P. Yang, *Advanced Composites and Hybrid Materials*, 2019, **2**, 201-213, doi: 10.1007/s42114-018-0066-x.
[33] S. Li, J. Sun, J. Guan, *Chinese Journal of Catalysis*, 2021, **42**, 511-556, doi: 10.1016/s1872-2067(20)63693-2.
[34] N. Karmodak, O. Andreussi, *ACS Energy Letters*, 2020, **5**, 885-891, doi: 10.1021/acsenergylett.9b02689.
[35] K. Huang, J. Liu, L. Wang, G. Chang, R. Wang, M. Lei, Y. Wang, Y. He, *Applied Surface Science*, 2019, **487**, 1145-1151, doi: 10.1016/j.apsusc.2019.05.183.
[36] W. Cheong, C. Liu, M. Jiang, H. Duan, D. Wang, C. Chen, Y. Li, *Nano Research*, 2016, **9**, 2244-2250, doi: 10.1007/s12274-016-1111-0.
[37] C. Tan, X. Cao, X. Wu, Q. He, Yang, X. Zhang, J. Chen, W. Zhao, S. Han, G. Nam, M. Sindoro, H. Zhang, *Chemical Reviews*, 2017, **117**, 6225-6331, doi: 10.1021/acs.chemrev.6b00558.
[38] H. Duan, N. Yan, R. Yu, C. Chang, G. Zhou, H. Hu, H. Rong, Z. Niu, J. Mao, H. Asakura, T. Tanaka, P. J. Dyson, J. Li, Y. Li, *Nature Communications*, 2014, **5**, 3093, doi: 10.1038/ncomms4093.
[39] A. Funatsu, H. Tateishi, K. Hatakeyama, Y. Fukunaga, T. Taniguchi, M. Koinuma, H. Matsuura, Y. Matsumoto, *Chemical Communications*, 2014, **50**, 8503-8506, doi: 10.1039/c4cc02527j.
[40] K. Huang, L. Zhang, T. Xu, H. Wei, R. Zhang, X. Zhang, B. Ge, M. Lei, J.. Ma, L.. Liu, H. Wu, *Nature Communications*, 2019, **10**, 606, doi: 10.1038/s41467-019-08484-8.
[41] H. Liu, P. Zhong, K. Liu, L. Han, H. Zheng, Y. Yin, C. Gao, *Chemical Science*, 2018, **9**, 398-404, doi: 10.1039/c7sc02997g.
[42] W. Mitchell, J. Xie, T. Jachimowski, W. Weinberg, *Journal of the American Chemical Society*, 1995, **117**, 2606-2617, doi: 10.1021/ja00114a025.
[43] K. Li, Y. Li, Y. Wang, J. Ge, C. Liu, W. Xing, *Energy & Environmental Science*, 2018, **11**, 1232-1239, doi: 10.1039/c8ee00402a.
[44] Z. Pu, I. Amiinu, Z. Kou, W. Li, S. Mu, *Angewandte Chemie International Edition*, 2017, **56**, 11559-11564, doi: 10.1002/anie.201704911.
[45] Y. Dang, T. Wu, H. Tan, J. Wang, C. Cui, P. Kerns, W. Zhao, L. Posada, L. Wen, S. L. Suib, *Energy & Environmental Science*, 2021, **14**, 5433-5443, doi: 10.1039/d1ee02380b.
[46] J. Zhang, Y. Zhao, X. Guo, C. Chen, C. Dong, R. Liu, C. Han, Y. Li, Y. Gogotsi, G. Wang, *Nature Catalysis*, 2018, **1**, 985-992, doi: 10.1038/s41929-018-0195-1.
[47] K. Huang, Z. Zhao, H. Du, P. Du, H. Wang, R. Wang, S. Lin, H. Wei, Y. Long, M. Lei, W. Guo, H. Wu, *ACS Sustainable Chemistry & Engineering*, 2020, **8**, 6905-6913, doi: 10.1021/acssuschemeng.0c00830.
[48] X. Qin, L. Zhang, G. Xu, S. Zhu, Q. Wang, M. Gu, X. Zhang, C. Sun, P. B. Balbuena, K. Amine, M. Shao, *ACS Catalysis*, 2019, **9**, 9614-9621, doi: 10.1021/acscatal.9b01744.
[49] K. Li, Y. Li, Y. Wang, J. Ge, C. Liu, W. Xing, *Energy & Environmental Science*, 2018, **11**, 1232-1239, doi: 10.1039/c8ee00402a.
[50] J. Mahmood, F. Li, S. Jung, M. Okyay, I. Ahmad, S. Kim, N. Park, H. Jeong, J. Baek, *Nature Nanotechnology*, 2017, **12**, 441-446, doi: 10.1038/nnano.2016.304.
[51] J. Zhang, P. Liu, G. Wang, P. Zhang, X. Zhuang, M. Chen, I. Weidinger, X. Feng, *Journal of Materials Chemistry A*, 2017, **5**, 25314-25318, doi: 10.1039/c7ta08764k.
[52] N. Mahmood, Y. Yao, J. Zhang, L. Pan, X. Zhang, J. Zou, *Advanced Science*, 2018, **5**, 1700464, doi: 10.1002/advs.201700464.
[53] B. Solanki, P. Ranjan, T. Chakraborty, M. Elik, *Engineered Science*, 2022, **19**, 83-88 doi: 10.30919/es8d684.
[54] H. Chang, Z. Liang, L. Wang, C. Wang, *Nanoscale*, 2022, **14**, 5639-5656, doi: 10.1039/D2NR00522K.
[55] Y. Zhu, X. Liu, S. Jin, H. Chen, W. Lee, M. Liu, Y. Chen, *Journal of Materials Chemistry A*, 2019, **7**, 5875-5897, doi: 10.1039/C8TA12477A.
[56] Q. Li, N. Li, J. An, H. Pang, *Inorganic Chemistry Frontiers*, 2020, **7**, 2089-2096, doi: 10.1039/d0qi00316f.
[57] Q. Feng, Z. Zhao, X. Yuan, H. Li, H. Wang, *Applied Catalysis B: Environmental*, 2020, **260**, 118176, doi: 10.1016/j.apcatb.2019.118176.
[58] C. Hu, L. Zhang, Z. Zhao, A. Li, X. Chang, J. Gong, *Advanced Materials*, 2018, **30**, 1705538, doi: 10.1002/adma.201705538.
[59] P. Du, K. Huang, X. Fan, J. Ma, N. Hussain, R. Wang, B. Deng, B. Ge, H. Tang, R. Zhang, M. Lei, H. Wu, *Nano Research*, 2022, **15**, 3065-3072, doi: 10.1007/s12274-021-3963-1.
[60] Y. Shi, B. Zhang, *Chemical Society Reviews*, 2016, **45**, 1529-1541, doi: 10.1039/c5cs00434a.
[61] J. Wang, W. Cui, Q. Liu, Z. Xing, A. M. Asiri, X. Sun, *Advanced Materials*, 2016, **28**, 215-230, doi: 10.1002/adma.201502696.
[62] S. Anantharaj, S. Kundu, S. Noda, *Journal of Materials Chemistry A*, 2020, **8**, 4174-4192, doi: 10.1039/c9ta14037a.
[63] K. Huang, R. Wang, H. Wu, H. Wang, X. He, H. Wei, S. Wang, R. Zhang, M. Lei, W. Guo, B. Ge, H. Wu, *Journal of Materials Chemistry A*, 2019, **7**, 25779-25784, doi: 10.1039/c9ta07469d.
[64] S. Anantharaj, S. Ede, K. Sakthikumar, K. Karthick, S. Mishra, S. Kundu, *ACS Catalysis*, 2016, **6**, 8069-8097, doi: 10.1021/acscatal.6b02479.

 

[65] Y. Liu, X. Li, Q. Zhang, W. Li, Y. Xie, H. Liu, L. Shang, Z. Liu, Z. Chen, L. Gu, Z. Tang, T. Zhang, S. Lu, *Angewandte Chemie International Edition*, 2020, **59**, 1718-1726, doi: 10.1002/anie.201913910.
[66] S. Sarwar, M. Lin, M. Ahasan, Y. Wang, R. Wang, X. Zhang, *Advanced Composites and Hybrid Materials*, 2022, **5**, 2339-2352, doi: 10.1007/s42114-022-00424-3.
[67] Y. Wang, D. Yao, Y. Zheng, *Advanced Composites and Hybrid Materials*, 2019, **2**, 608-625, doi: 10.1007/s42114-019-00125-4.
[68] P. Bag, G. Singh, S. Singha, G. Roymahapatra, *Engineered Science*, 2021, **13**, 1-10, doi: 10.30919/es8d1166.
[69] R. Xue, H. Guo, W. Yang, S. Huang, G. Yang, *Advanced Composites and Hybrid Materials*, 2022, **5**, 1595-1611, doi: 10.1007/s42114-022-00432-3.
[70] W. Zhang, P. Yang, *Advanced Composites and Hybrid Materials*, 2019, **2**, 201-213, doi: 10.1007/s42114-018-0066-x.
[71] J. Zhang, X. Qu, Y. Han, L. Shen, S. Yin, G. Li, Y. Jiang, S. Sun, *Applied Catalysis B: Environmental*, 2020, **263**, 118345, doi: 10.1016/j.apcatb.2019.118345.
[72] M. Luo, J. Cai, J. Zou, Z. Jiang, G. Wang, X. Kang, *Journal of Materials Chemistry A*, 2021, **9**, 14941-14947, doi: 10.1039/d1ta03593b.
[73] K. Peng, N. Bhuvanendran, S. Ravichandran, W. Zhang, Q. Ma, Q. Xu, L. Xing, L. Khotseng, H. Su, *International Journal of Hydrogen Energy*, 2020, **45**, 30455-30462, doi: 10.1016/j.ijhydene.2020.08.060.
[74] H. Zhao, J. Liang, Q. Zheng, *Ionics*, 2022, **28**, 839-848, doi: 10.1007/s11581-021-04377-3.
[75] X. Wang, G. Huang, Z. Pan, S. Kang, S. Ma, P. Shen, J. Zhu, *Chemical Engineering Journal*, 2022, **428**, 131190, doi: 10.1016/j.cej.2021.131190.
[76] J. Wei, M. Cao, K. Xiao, X. Guo, S. Ye, Z. Liu, *Small Structures*, 2021, **2**, 2100047, doi: 10.1002/sstr.202100047.

## Author Information

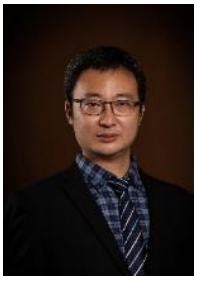

***Xuchao Pan*** *received his ph.D. from Nanjing university of science and technology in 2013. Now he is research associate in Nanjing university of science and technology. He has been engaged in the magnetic materials, functional materials in engineering.*

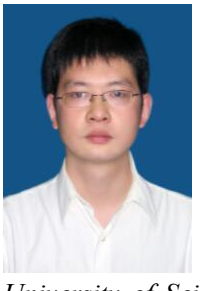

***Ming Lei*** *received his M.D. at State Key Laboratory of Materials Composites and Advanced Technology, Wuhan University of Technology in 2004. Then, he received his Ph.D. from the Laboratory of Nanophysics and Devices, Institute of Physics, Chinese Academy of Sciences in 2007. He worked as a postdoctoral fellow at The Hong Kong University of Science and Technology (2007-2008) and the Chinese University of Hong Kong (2009-2010). He is now a professor and doctoral supervisor of the School of Science, Beijing University of Posts and Telecommunications. He has long been engaged in the preparation of low dimensional nano materials, photoelectric properties and device applications.*